

CHANGES IN WETTABILITY STATE DUE TO WATERFLOODING

Andrew Fogden, Evgenia V. Lebedeva

Dept of Applied Mathematics, Australian National University, Canberra, Australia

This paper was prepared for presentation at the International Symposium of the Society of Core Analysts held in Austin, Texas, USA 18-21 September, 2011

ABSTRACT

Some literature coreflood data point to the initial wettability state undergoing change during waterflooding, usually towards water-wetness. The current study aimed to directly probe the adsorbed/deposited oil components on model silicate substrates prior to and after flooding. Bare glass and kaolinite-coated glass in the initial brine were drained with crude oil and aged, after which the oil was displaced with the flooding brine. For a matrix of initial and flood brines (comprising sodium and calcium) of varying salinity and/or pH, the oil remaining on the substrates was analyzed by high resolution scanning electron microscopy, contact angle and spectroscopy. On glass, the oil layer contacting it in the initial (aged) state retracts and detaches during flooding, to typically leave individual oil nano-droplets separated by clean substrate. Brines less able to overcome the oil-glass adhesion displayed a higher coverage of more irregularly shaped, semi-retracted droplets and a higher frequency of larger microscopic residues. On kaolinite-coated glass, the added porosity and roughness increased the presence of these adhering, stranded residues. On glass, the residual deposit after high salinity flooding is generally least at intermediate flood pH 6, while residues decrease with decreasing pH of low salinity floods. However, on kaolinite-coated substrates, residual deposit is greatest after flooding at intermediate pH 6, and also increases on reduction of flood salinity.

INTRODUCTION

During reservoir formation, drainage of pore-filling brine by the accumulating crude oil causes local alteration of naturally water-wet pore walls towards oil-wetness, if the water thin film lining the mineral ruptures to allow adsorption or deposition of oil polar components, namely asphaltenes and resins. Tighter pore confines can retain bulk brine and thus their water-wetness, giving rise to the mixed-wet state. The distribution of polar components at the pore- and molecular scales in this initial state, and their effect on local oil-brine contact angles at walls, would be valuable input into development of more systematic strategies for optimizing oil recovery by waterflooding. To this end, many studies have prepared smooth model substrates of quartz, mica and glass in initial wettability states by oil drainage of surrounding brine and aging, for measurement of macroscopic contact angles or nanoscopic imaging of adsorbed/deposited asphaltenics using atomic force microscopy [1-3]. This work evidenced the strong effect of brine composition on wettability alteration, with low concentration and pH favoring oil-wetness and high concentration and pH helping to preserve water-wetness.

Recent progress has been made in imaging and quantifying the initial wettability of more complex model systems containing pores. Asphaltenic adsorbates/deposits are amenable to imaging via the common and versatile technique of scanning electron microscopy (SEM), removing the limitation to flat, impervious substrates. Drainage of a macroporous glass bead pack gave distributions consistent with the mixed-wet picture of reservoirs [4]. Other studies used flat substrates coated with layers of nanoporous silica [5] or kaolinite [6,7] to show that crude oil can spontaneously displace brine from the submicron pores to alter wettability, depending on brine composition and local pore surface chemistry.

Modeling of waterflooding typically presumes that the initial wettability is unaffected by the evolution in pore occupancies during recovery. However, mounting evidence from core floods suggests that rock surfaces can undergo *in situ* change. These changes, often reverting towards a more water-wet state, are proposed to underpin enhanced recovery by lowering the salinity of the flood [8,9] or re-injecting oil and re-flooding [10]. The above-mentioned SEM-based analyses have been extended to imaging pore-scale effects of reduced salinity in Berea sandstone [11]. This study showed substantial oil-mediated mobilization of mineral fines during flooding, however their migration complicated the assessment of wettability changes. More recent work returned to flat glass substrates, showing that the oil at the surface remains fluid-like, and is able to retract and detach nanoscopically during flooding [12]. The current study extends this by addressing both glass and kaolinite-coated glass in their initial wettability state and after flooding, for a matrix of brines, including high and low salinity, and imposed variations in pH from initial to flooded states. While broadly relevant to oil recovery from sandstones, the study also seeks to determine whether reduced salinity *per se*, or the pH shift it can induce via ion exchange or dissolution, is more capable of changing wettability of grains and clays.

EXPERIMENTAL

Substrates, Oil and Brines

The two types of model substrate used were cleaned microscope glass slides without or with a ~ 1 μm thick coat of kaolinite (KGa-1b, Clay Minerals Society) applied via a published method [6,7]. The oil was an asphaltic crude, designated as WP, with density 0.9125 gcm^{-3} , viscosity 111 $\text{mPa}\cdot\text{s}$, n-C₆ asphaltene content 6.3 wt%, and acid and base numbers 1.46 and 2.49 mg KOH/g oil (all at 22°C) [10]. Brines for the initial state (i.e. connate, drained by oil) and for flooding (displacing oil) all comprised 90 wt% NaCl and 10 wt% CaCl₂, dissolved in deionized water (from a Millipore Milli-Q system) to total concentrations of 50 or 1 g/l . Each was degassed and prepared at three pH values, namely unadjusted (pH 5.9 ± 0.2) or adjusted to 4.0 ± 0.1 with HCl or 9.0 ± 0.2 with NaOH. Zeta potentials of ground glass slide, kaolinite powder and crude oil were measured in the brines using a Zetasizer Nano-ZS (Malvern Instruments), and are listed in Table 1.

Creation and Analysis of Wettability States

The procedures for draining, aging, flooding and solvent rinsing the model substrates are based on a recent publication [12]. A piece (7×26 mm^2) of the bare or kaolinite-coated glass was equilibrated in the initial brine, with the oil on top, in a vial for 6 h at room

temperature. The bulk brine was then removed by pipette and the oil-immersed substrate was further drained of its enveloping water by centrifuging the vial at 3000 rpm for 10 min., followed by aging at 60°C for 30 ± 2 days. Substrates in this initial state post-aging were waterflooded at 60°C using a syringe pump to inject the flooding brine into the vial bottom at 2.5 cm³/h for 1 h, thus raising the bulk oil level above the substrate. The vial was centrifuged at 3000 rpm for 10 min. to strip any large oil drops adhering to the substrate, and the oil above was removed by pipette. The centrifugation was repeated, and oil remaining at the air interface was removed by tissue. The substrate thus flooded was transferred to methanol for 10 min, to remove salt, and dried ambiently. Flooding was not performed for some samples, to examine the initial wettability state. This necessitates removal of the surrounding bulk oil with organic solvent, for which decalin was chosen, as it least disturbs the polar components adsorbed/deposited on the substrate. The aged substrate was thus transferred to decalin for 20 min., and then to fresh decalin for 2 h (remaining colorless), followed by the above-mentioned methanol rinsing step, and drying under light vacuum for 3 h at room temperature. Some flooded kaolinite-coated glass samples were also rinsed using these same decalin/methanol steps to remove non-adsorbed/deposited components prior to fluorescence spectroscopy (see below).

Table 1. Zeta potential of glass, kaolinite and oil in the six brines, at the two salinities for three pH values.

Brine conc., g/l	Brine pH	Glass, mV	Kaolinite, mV	WP crude, mV
50	4	-5.8	-2.8	-3.4
50	6	-9.1	-5.0	-6.2
50	9	-8.3	-4.8	-9.0
1	4	-30.4	5.8	31.3
1	6	-40.9	-4.4	-7.1
1	9	-38.3	-26.1	-25.7

The matrix of samples for analysis of their initial wettability state (drained and aged, but not flooded) used the 50 or 1 g/l brine, at pH 4, 6 or 9 for bare glass, or only pH 6 for kaolinite-coated glass. For each salinity-pH-substrate combination, two replicates were prepared; one for imaging by field emission scanning electron microscopy (FESEM) and the other for contact angle measurement (glass substrates) or fluorescence spectroscopy (kaolinite-coated glass). The matrix for analysis of the flooded wettability state used as initial brine the 50 g/l solution, again at pH 4, 6 or 9 for bare glass or only pH 6 for kaolinite-coated glass. Flooding was performed with the 50 or 1 g/l brine at pH 4, 6 or 9. Again, a replicate pair was prepared for each initial/flooding salinity-pH-substrate combination; one (methanol rinsed) for FESEM imaging and the other for contact angle (methanol-rinsed glass) or spectroscopy (decalin/methanol-rinsed, kaolinite-coated glass).

The three analyses are similar to previous studies and are briefly summarized. Oil deposit imaging was performed using FESEM (Zeiss UltraPlus Analytical) under high vacuum in secondary electron mode at 1 kV, with the substrates lightly sputter coated with platinum [6,7,12]. All contact angle measurements [6,7,12] were performed at 23-24°C using a

contact angle goniometer (KSV Instruments) for a captive pendant drop of the crude oil on the glass samples in their pre-prepared wettability states. The surrounding solution matched the initial brine (for non-flooded samples) or flooding brine. The pumped-out drop was left in the brine for 2 min, and then contacted with the substrate to measure water-receding and -advancing angles through the brine directly after drop growth and retraction, respectively. The duration of substrate contact was also 2 min, which allows some drop adhesion to the preexisting oil deposits, but helps avoid new deposition during measurement. The procedure was duplicated for 3 or 6 drops per non-flooded or flooded sample. For kaolinite-coated samples, a FluoroMax-3 spectrofluorometer (Horiba Jobin Yvon) was used to determine the total amount of adsorbed/deposited asphaltenic components via their natural fluorescence [7]. To this end, all substrates (non-flooded or flooded) were decalin/methanol rinsed, and their uncoated back sides cleaned, to remove all but the asphaltenics adsorbed/deposited on the coat. These residues were extracted by soaking in 3.1 g of azeotropic chloroform/methanol blend at 50°C for 24 h. The solutions were analyzed in a quartz cuvette (10x10x40 mm³; Starna Cells) to record emission spectra over 380-560 nm from 340 nm excitation. In separate experiments, the asphaltene fraction of the oil was isolated by heptane precipitation, from which asphaltene solutions of known concentration were prepared in this same solvent blend. Their fluorescence was analyzed similarly to calibrate intensities of sample extracts to concentration.

RESULTS AND DISCUSSION

Wettability of Glass

FESEM micrographs of the oil deposits remaining on the glass substrates after drainage and aging, without or with subsequent flooding, and solvent post-rinsing (as described above), were acquired using fixed high magnification at 16 sites over each of the 24 samples. While FESEM cannot give height information, image analysis of the deposits (which typically appear lighter than their glass background) provided several metrics of their 2D lateral features. ImageJ software yielded the three measures of coverage (percentage of substrate area occupied by deposit), particle area (base area of individual deposit particles contacting the substrate) and particle circularity (ratio of this particle base area to the area of a circle with this perimeter). The average and standard deviation were calculated from all images for each sample. The micrographs shown below are among the most representative members of their image sets with respect to all averaged measures. Figure 1 presents micrographs of the initial wettability state established in the 50 or 1 g/l brine at pH 6 (post-rinsed in decalin and methanol). Figure 2 shows images of the flooded wettability state using the 50 g/l solution as both initial and flooding brine for all nine combinations of initial/flood pH (and methanol post-rinsed). Figure 3 plots the receding and advancing contact angles on the full set of similarly prepared sister samples, for the initial wettability state (a) and after flooding (c-d). In Fig. 3b, these angles are compared to the corresponding values of the FESEM image analysis metric giving best correlation, namely deposit circularity. In this graph, circularity, C , is re-plotted as acircularity, $1 - C$, so that 0 would correspond to a perfectly circular deposit particle base and values towards 1 signify increasingly irregular, non-compact base shapes.

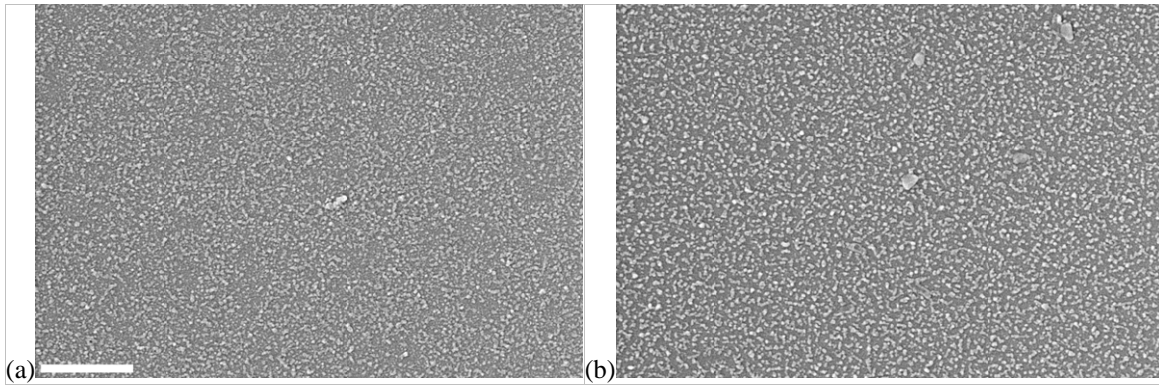


Figure 1. FESEM images of oil deposits on glass for the (a) high and (b) low salinity initial brine, both at pH 6, and without flooding. Images are $3.0 \times 2.0 \mu\text{m}^2$; the scale bar in (a) is 500 nm and applies to both.

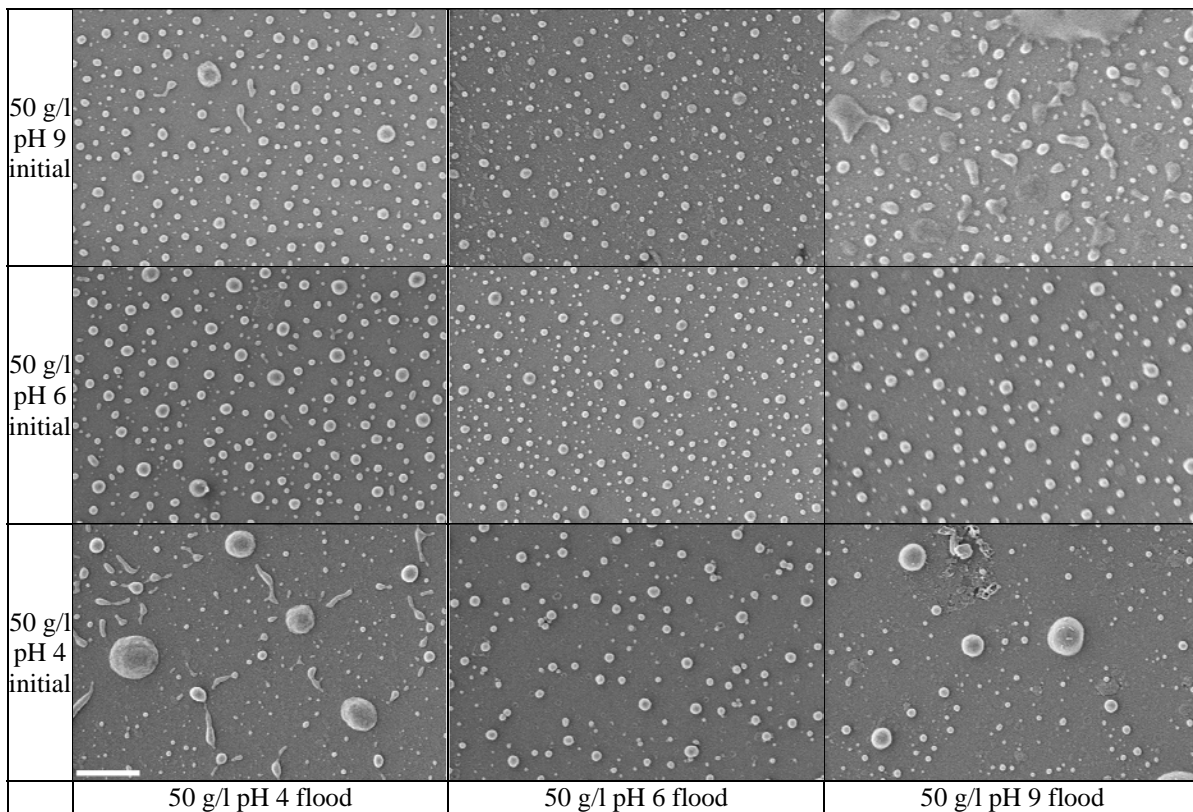


Figure 2. FESEM images of oil deposits remaining on glass for the nine pH combinations of the 50 g/l initial brine (rows) and 50 g/l flooding brine (columns). Images are $3.0 \times 2.0 \mu\text{m}^2$; the scale bar in the bottom left image is 500 nm and applies to all.

Flooding strips the vast majority of macroscopic bulk oil from the glass, further aided by subsequent centrifugation, so imaging and contact angle measurement do not need the extra step of decalin post-rinsing required for analysis of initial wettability. Flooded samples (Fig. 2) thus retain all adhering nano/micro-scopic oil components, while non-flooded samples (Fig. 1) keep only the adsorbate/deposit, i.e. the adhering oil footprint.

Although the term oil “deposit” will be used for both prepared states, the two cannot be directly compared. On flooded samples, contact angle runs in which the pendant oil drop encountered larger microscopic residue(s) gave very high receding angle (above 80°, with correspondingly high advancing angle). In these occasional cases the pendant drop does not measure substrate wettability; accordingly, such data were excluded from Fig. 3.

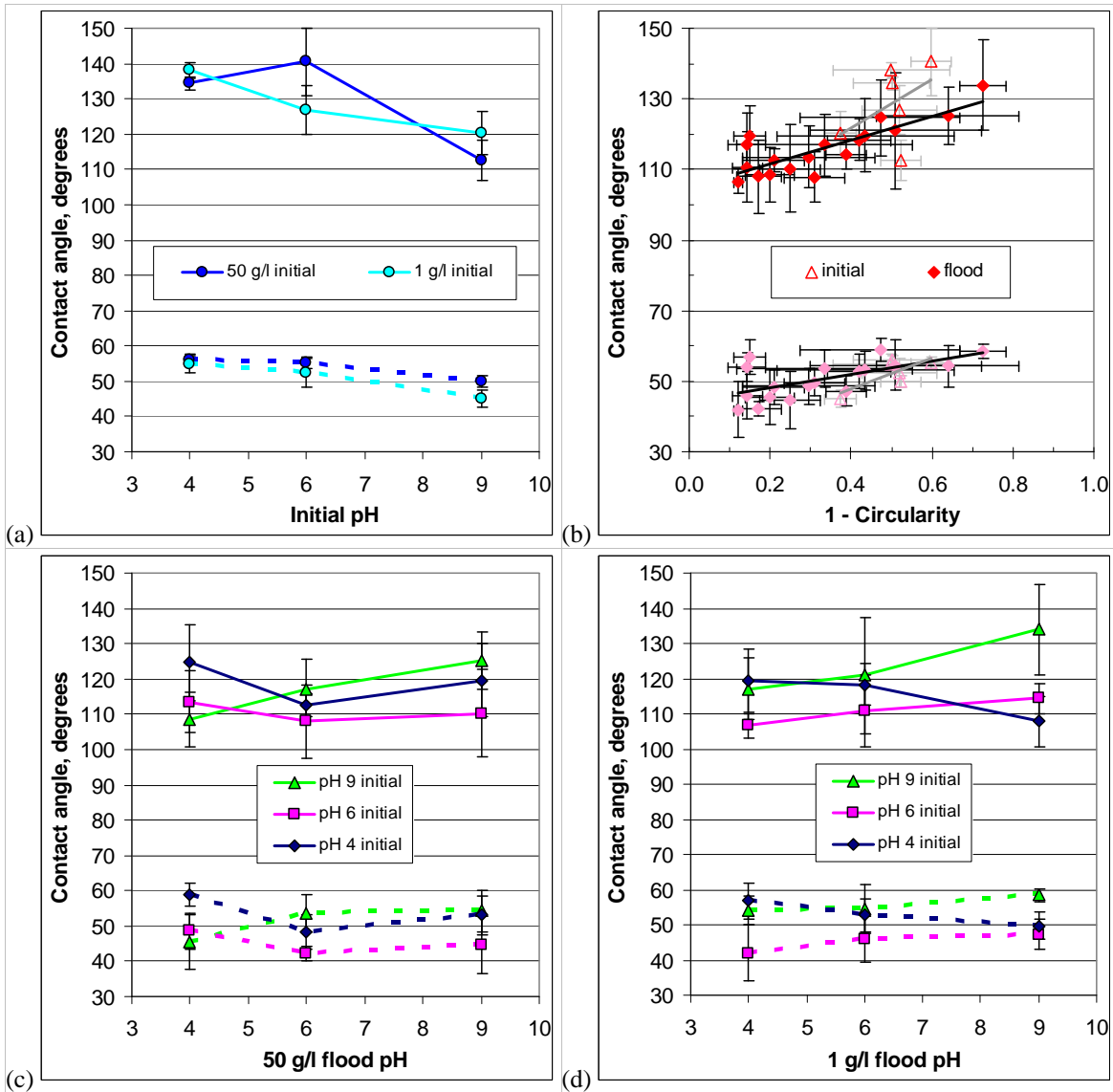


Figure 3. Receding (lower, dashed line curves) and advancing (upper, solid line curves) angles of oil drops on glass pretreated to its (a) initial or (c-d) flooded wettability state, in the corresponding initial or flooding brine. The sets of curves are for the differing (a) salinity or (c-d) pH of the initial brine in the legends. In (b), all angles on initial or flooded wettability samples are plotted versus deposit acircularity from FESEM.

Consider first the initial wettability state. In all cases the deposits appear qualitatively as in Fig. 1, comprising asphaltenic aggregates separated by nano/micro-scopic gaps due to brine trapped under the collapsing oil interface [3,4,12]. The three image analysis metrics

verify the relatively high coverage of small, irregular (acircular) particles. Further, they exhibit a peak at pH 6 for both salinities, so deposition is most complete for the samples in Fig. 1 and decreases for lower or higher pH, with least deposit for 1 g/l brine at pH 9. According to the contact angles on these deposit-bearing substrates in Fig. 3a, all samples are oil-wet, although both receding and advancing angles tend to decrease with pH. These angles are dictated by the 1) pre-existing deposit, and 2) ability of the oil pendant drop to re-establish molecular contact with it. The second contribution is governed by DLVO theory [1,12] of interactions on interfacial approach, for which the zeta potentials (Table 1) favor contact angle decrease with pH. Glass and oil are more strongly anionic at higher pH via acid group deprotonation, thus repelling across brine to hinder contact. While glass remains anionic at pH 4, oil displays greater cationicity via base group protonation and calcium ion binding, favoring attraction and contact. On the other hand, the extent of deposit is dictated by non-DLVO interactions of slow reconfiguration of aggregated polar components during aging. The peak in deposition at pH 6 presumably reflects the excessive brine trapping due to either too weak attraction (pH 9) or too strong attraction prohibiting interfacial rearrangement for drainage (pH 4). The angle data is a convolution of these two contributions, generally decreasing with pH but tending to peak at pH 6.

In the flooded state, the FESEM images on glass (Fig. 2) generally depict a scattering of discrete nanoscale oil droplets with smooth, fluidic appearance. Lower magnification images more clearly show that their distribution is not random; the nano-droplets tend to be arranged in 1D trails which, on joining the dots, form a 2D foam-like superstructure. This suggests that on flooding, the advancing water increasingly perforates the oil film at the substrate, partly by swelling the trapped brine nano-channels. The surface oil retracts and detaches, taking the adsorbed/deposited asphaltenics with it, and the holey film decomposes into foam-like struts, which further decompose into the nano-droplets due to Rayleigh instability. These observations agree with the previous study [12]. Control experiments without post-flooding centrifugation showed the same texture, verifying that it results from flooding. For brines less able to overcome the oil-substrate adhesion, this decomposition and detachment is curtailed. The bottom left and top right images in Fig. 2 show incomplete foam retraction and strut break-up, also with flatter, less fluidic deposits of irregular shape remaining attached after detachment of the associated bulk oil.

The corresponding contact angles on the flooded samples in Fig. 3c-d show variations up to 17° and 27° in receding and advancing angle averages, depending on initial/flood pH and salinity. The standard deviations (error bars) average 5° and 9° , respectively, thus pendant drop measurements present limitations for quantifying the relatively subtle changes in contact angle expected from flooding. Owing to these general limitations, the current study addressed a substantial matrix of brines, also supported by FESEM imaging and analysis. It could be expected that small contact angles are associated with relatively low deposit coverage, low particle (drop) size and low acircularity, while large angles tend to the opposite extremes. This is borne out by the results; in particular, acircularity exhibits the strongest correlation to the contact angle data (Fig. 3b), since clean, compact retraction of nano-droplets favors similar behavior for the macroscopic pendant drop.

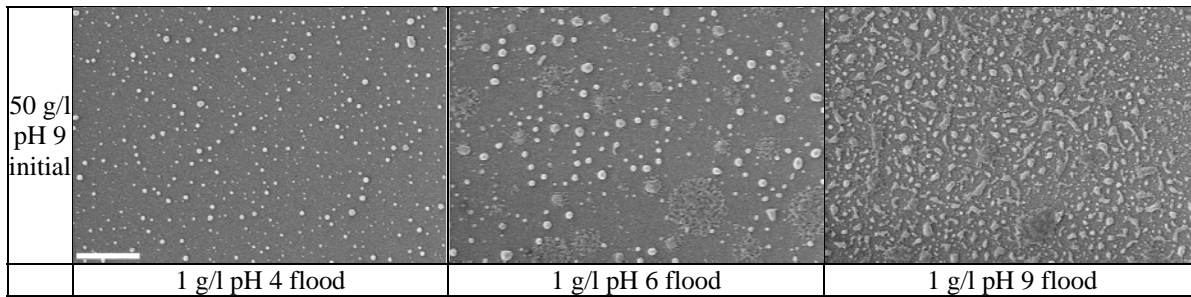


Figure 4. FESEM images of deposits remaining on glass for the initial brine of 50 g/l at pH 9, flooded with 1 g/l at pH 4, 6 or 9. Images are $3.0 \times 2.0 \mu\text{m}^2$; the scale bar in the left image is 500 nm and applies to all.

Increase in pH of the 50 g/l flood from 4 to 6 (left to middle columns in Fig. 2) tends to reduce the residual deposit. This is in line with the above-mentioned decrease in oil-glass adhesion with pH, and the enhanced scope for rearrangement of deposits (now aiding their removal) under the milder interactions at pH 6. However, further reduction in adhesion from flood pH 6 to 9 (middle to right columns in Fig. 2) gives greater residuals. The increased oil-glass repulsion likely promotes rapid swelling of trapped brine ahead of the advancing bulk meniscus. This brine precursor film thickening can disconnect oil at the substrate from bulk oil, limiting the ability of the bulk meniscus to remove it. The 1 g/l floods are somewhat similar, however for all initial-state pH values, the residuals are not minimized at pH 6, but rather increase with flood pH. Figure 4 shows this for the case of initial pH 9. Reduction in flood salinity increases oil-glass electrostatic interactions (Table 1) and exerts an extra osmotic pressure to swell the initially high-salinity trapped brine. Precursor film thickening is thus likely to be more prevalent for the 1 g/l floods, so oil-glass attraction at lower flood pH is more necessary to resist the overwhelming drive to prematurely disconnect surface oil. Receding and advancing contact angles on the post-flooded substrate in Figs. 3c-d are well correlated to each other, and to deposit acircularity in Fig. 3b. The angles are thus dictated by the pre-existing residues, plus the extra contribution from DLVO interactions governing reestablishment of oil drop contact with residues in the flood solution. For the 50 g/l floods, these interactions are weaker. The angles thus mirror the deposit trends, with a minimum at flood pH 6, aside from the cases at initial pH 9 most prone to film thickening, for which the minimum shifts to flood pH 4 as explained above. For the 1 g/l floods, the contact contribution is stronger and tends to oppose the deposit trends. For example, at initial pH 4, residues increase with flood pH due to film thickening, however contact angles in Fig. 3d decrease with flood pH due to the strong attraction driving contact (pH 4) or repulsion hindering it (pH 9).

Wettability of Kaolinite-Coated Glass

The study of kaolinite-coated glass followed similar lines to that described above for bare glass, with some differences. The matrix of brines was reduced by limiting the initial state to only pH 6. The sample preparation for FESEM and the imaging were identical. However, for the porous coats of multiple layers of kaolinite platelets, not all deposits are visible from the surface images, and those which are cannot readily be segmented from the platelets for image analysis. Representative images are given in Fig. 5 for the initial

wettability state (decalin/methanol post-rinsed) and Fig. 6 for the flooded state (methanol post-rinsed). The sister samples were not used for contact angle analysis, as adhesion of the pendant drop would be underestimated, if not given sufficient time to reestablish nanoscopic connections to subsurface deposits, or overestimated, if connecting to larger oil micro-droplets or puddles remaining at the surface after centrifugation. Instead, the total amount of adsorbed/deposited asphaltenics (after decalin/methanol post-rinsing) was determined by solvent extraction for fluorescence spectroscopy. Emission intensity difference at 499 nm was calibrated to asphaltenic concentration and in turn to deposit mass per planar area of the glass piece, plotted in Fig. 7 for the six flooded samples.

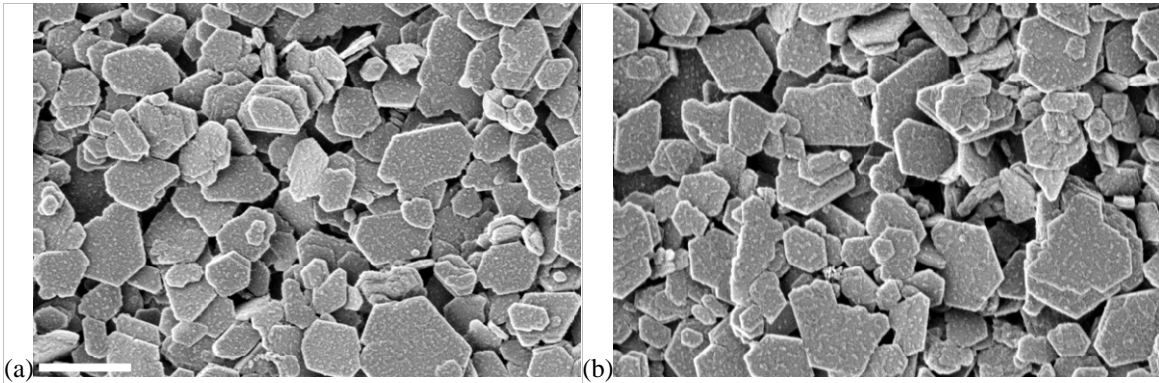


Figure 5. FESEM images of deposits on kaolinite-coated glass for (a) high and (b) low salinity initial brine, both at pH 6, without flooding. Images are $3.0 \times 2.0 \mu\text{m}^2$; the scale bar in (a) is 500 nm and applies to both.

For the initial wettability in Fig. 5, all visible platelet faces bear asphaltenic nanoparticle aggregates separated by uncovered nanodomains, similar to the textures on glass (Fig. 1). In occasional darker locations revealing underlying glass through inter-kaolinite pores (e.g. near the left edges in Fig. 5a-b), it too bears deposit. Thus oil spontaneously infiltrates the coat during aging to displace brine and alter wettability, as seen in other studies [7]. Platelet edges remain relatively free from deposit. No significant differences in deposition are apparent for these two salinities, as was also the case for bare glass. This similarity is confirmed by spectroscopy; the deposit mass per planar area for the 50 and 1 g/l initial brines (at pH 6) is 6.0 and 5.3 mg/m^2 . From Table 1, the zeta potentials of kaolinite and oil in both brines are all very similar (slightly net negative) at pH 6, as this is close to their crossover to cationicity. Thus both surfaces possess substantial densities of deprotonated acid groups, protonated base groups and calcium-bound sites, sufficient for local attraction of oppositely charged patches and faces to alter wettability.

All flooded samples (Fig. 6) were prepared from the same initial state for the 50 g/l brine at pH 6, with wettability corresponding to Fig. 5a, although again no comparison between Figs. 5 and 6 is possible due to their differing post-rinsing. The deposits in Fig. 6 are fluidic and often comprise nano-droplets, however the porous, comparatively rough and heterogeneous kaolinite coats limit the completeness of oil retraction and detachment, leading to more irregularly shaped droplets and more frequent larger blobs. The 50 g/l flood at pH 4 in Fig. 6 exhibits isolated nano-droplets on platelet faces, and also tendril-

shaped analogs lining edges, while the inter-kaolinite pores are mainly vacant. For the 50 g/l flood at pH 9, deposits are somewhat more prevalent, as nano-droplets on faces and larger blobs stranded in pores. For the 50 g/l flood at pH 6, oil films cover many platelets and substantially fill pores, smothering much of the angular features of the coat. The corresponding images in Fig. 6 for the 1 g/l flood show similar trends in pH, although in each case with systematically greater residuals than for 50 g/l flooding. This qualitative hierarchy from FESEM images is consistent with the deposit mass per planar area from spectroscopy in Fig. 7. For both flood salinities, the amount of asphaltenics remaining is greatest at pH 6, and decreases substantially for the lower and higher pH floods. Compared at the same pH, the low salinity flood systematically retains more deposit.

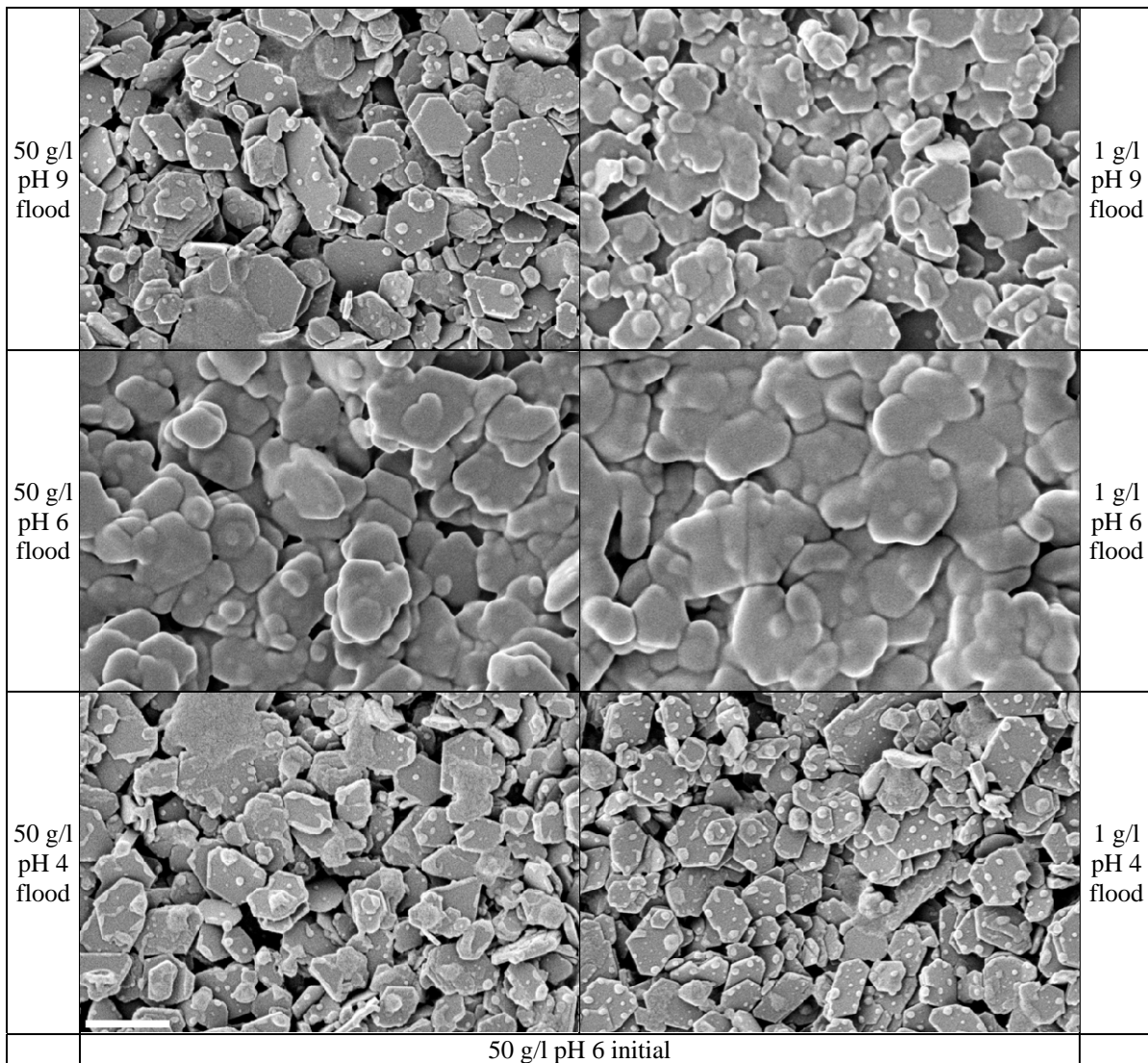


Figure 6. FESEM images of deposits remaining on kaolinite-coated glass after flooding of the same initial state (in 50 g/l brine at pH 6) with either the high (left column) or low (right) salinity brine at the three pH values. Images are $3.0 \times 2.0 \mu\text{m}^2$; the scale bar in the bottom left image is 500 nm and applies to all.

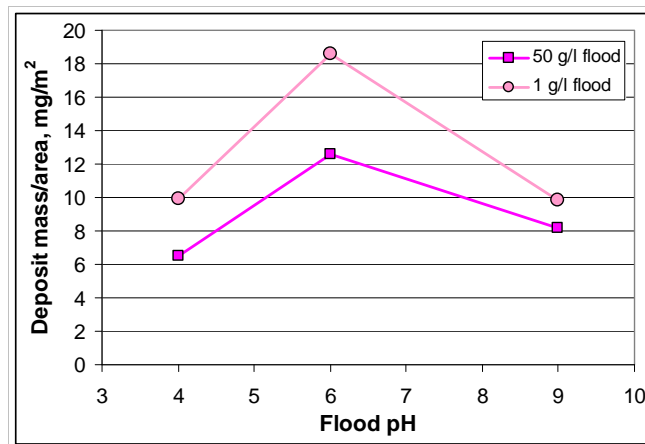


Figure 7. Total mass of asphaltenic deposits remaining, per planar area of kaolinite-coated slide, for the six flooded samples, all starting from the same initial wettability state (in 50 g/l brine at pH 6).

The results could be explained by 1) non-equilibrium or 2) equilibrium mechanisms. First, the fact that residual deposit is largest when the flood pH matches that of the oil-wet initial state (pH 6) suggests that pH perturbation of acid-base adhesive interactions from their pre-equilibrated initial state during flooding is responsible for oil removal. Second, the change in flood pH renders the zeta potentials of both interfaces in Table 1 either more negative (pH 9) or more positive (pH 4), and thus more repulsive. Increased removal at these extreme pH values is thus also expected if the oil-kaolinite interactions re-equilibrate to the flood pH. For both explanations the greater residual for low salinity flooding may appear somewhat incongruous, as this increases both the perturbation of the initial state and the strength of the similarly-signed interfacial charges in equilibrium at pH 4 and 9. However, previous studies [6,7] showed that decreased salinity of sodium-calcium brines typically increases short-time adhesion and longer-time deposition of oil on kaolinite, in agreement with Figs. 6-7, by aiding local attraction of oppositely charged patches on the two interfaces, even if both net zeta potentials are of the same sign. The extra osmotic pressure contribution swelling the brine trapped in the coat when exposed to the 1 g/l floods may also disconnect oil in/on the coat from bulk oil to limit removal, as discussed above for glass. It should be reemphasized that initial and flooded wettability states cannot be directly compared, in spite of both states being decalin/methanol post-rinsed and similarly analyzed by spectroscopy. The above-mentioned deposit masses in the initial state are actually lower than in Fig. 7. Extraneous deposition occurs when flooded substrates are decalin rinsed, due to precipitation of asphaltenics adsorbed at oil-brine interfaces. All values in Fig. 7 are thus overestimates, as shown in other work [12].

CONCLUSION

Models of oil recovery in which asphaltenic films, deposited on wettability-altered pore subareas in the initial reservoir state, are assumed to be solid-like and unresponsive to flooding, while bulk oil is cleanly removed, are too simplistic. Oil remains fluidic, even across the nanometers closest to the mineral substrate, and can retract and detach during flooding, carrying the adsorbed species with it. The flooded wettability state typically

comprises a partial coverage of scattered nano-droplets. For silicate model substrates, the residues depend on both flood salinity and pH. On glass, increased flood pH can lead to greater retention of deposit, and yet still exhibit relatively weak adhesion of bulk oil, due to disconnection by precursor film thickening. This is favored for low salinity floods. For kaolinite-coated glass, increase or decrease of flood pH from initially neutral conditions led to decrease in residues, while reduced salinity increased residues. However, in clay-rich sandstones, low salinity flooding may perturb the brine pH from its initial rock-buffered value, to counteract this direct effect of salinity on wettability. Along with the scattered nano-droplets, oil recovery also leaves larger microscopic oil remnants on pore walls, even for slow floods on smooth glass, so subsequent re-exposure of a flooded pore to oil must be described as a receding meniscus simultaneously undergoing reconnection.

ACKNOWLEDGEMENTS

The member companies of the Digital Core Consortium Wettability Satellite are thanked for financial support. A.F. was supported by an ARC Discovery Grant.

REFERENCES

1. Buckley, J.S.; Takamura, K.; Morrow, N.R. Influence of electrical surface charges on the wetting properties of crude oils. *SPE Res. Eng.* **1989**, 332-340.
2. Yang, S.-Y.; Hirasaki, G. J.; Basu, S.; Vaidya, R. Mechanisms for contact angle hysteresis and advancing contact angles. *J. Pet. Sci. Eng.* **1999**, 24, 63-73.
3. Freer, E.M.; Svitova, T.; Radke, C.J. The role of interfacial rheology in reservoir mixed wettability, *J. Pet. Sci. Eng.* **2003**, 39, 137-158.
4. Kumar, M.; Fogden, A. Patterned wettability of oil and water in porous media. *Langmuir* **2010**, 26, 4036-4047.
5. Fogden, A. Experimental investigation of deposition of crude oil components in brine-filled pores. *Petrophysics* **2010**, 51, 399-407.
6. Lebedeva, E.V.; Fogden, A. Adhesion of oil to kaolinite in water. *Environ. Sci. Technol.* **2010**, 44, 9470-9475.
7. Lebedeva, E.V.; Fogden, A. Wettability alteration of kaolinite exposed to crude oil in salt solutions. *Colloids Surf. A* **2011**, 377, 115-122.
8. Lager, A.; Webb, K.J.; Black, C.J.J.; Singleton, M.; Sorbie, K.S. Low salinity oil recovery - an experimental investigation. *Petrophysics* **2008**, 49, 28-35.
9. Wideroe, H.C.; Rueslaatten, H.; Boassen, T. et al. Investigation of low salinity water flooding by NMR and CryoESEM. *Proceedings of the 2010 International Symposium of the Society of Core Analysts*; Halifax, Canada, Oct 4-7, 2010; Paper 2010-26.
10. Loahardjo, N.; Xie, X.; Morrow, N.R. Oil recovery by sequential waterflooding of mixed-wet sandstone and limestone. *Energy Fuels* **2010**, 24, 5073-5080.
11. Fogden, A.; Kumar, M.; Morrow, N.R.; Buckley, J.S. Mobilization of fine particles during flooding of sandstones and possible relations to enhanced oil recovery. *Energy Fuels* **2011**, 25, 1605-1616.
12. Lebedeva, E.V.; Fogden, A. Nano-scale structure of crude oil deposits on water-wet substrates: Dependence on aqueous phase and organic solvents. *Colloids Surf. A* **2011**, 380, 280-291.